Reconfigurable Intelligent Surfaces for Smart Wireless Environments: Channel Estimation, System Design, and Applications in 6G Networks

Ying-Chang Liang, Jie Chen, Ruizhe Long, Zhen-Qing He, Xianqi Lin, Chenlu Huang, Shilin Liu, Sherman Shen, Marco Di Renzo

SCIENCE CHINA
Information Sciences

• **RESEARCH PAPER** •

Reconfigurable Intelligent Surfaces for Smart Wireless Environments: Channel Estimation, System Design and Applications in 6G Networks

Ying-Chang LIANG[1*], Jie CHEN[1], Ruizhe LONG[1], Zhen-Qing HE[1], Xianqi LIN[2], Chenlu HUANG[2], Shilin LIU[2], Xuemin (Sherman) SHEN[3] & Marco Di RENZO[4]

[1] *Center for Intelligent Networking and Communications, University of Electronic Science and Technology of China, Chengdu, 611731, China*
[2] *School of Electronic Science and Engineering, University of Electronic Science and Technology of China, Chengdu, 611731, China*
[3] *Department of Electrical and Computer Engineering, University of Waterloo, Waterloo, N2L 3G1, Canada*
[4] *CNRS, CentraleSupélec, Laboratoire des Signaux et Systèmes, Université Paris-Saclay, 3 Rue Joliot-Curie, 91192 Gif-sur-Yvette, France*

Abstract Reconfigurable intelligent surface (RIS), one of the key enablers for the sixth-generation (6G) mobile communication networks, is considered by designers to smartly reconfigure the wireless propagation environment in a controllable and programmable manner. Specifically, RIS consists of a large number of low-cost and passive reflective elements (REs) without radio frequency chains. The system gain of RIS wireless systems can be achieved by adjusting the phase shifts and amplitudes of REs so that the desired signals can be added constructively at the receiver. However, RIS typically has limited signal processing capability and cannot perform active transmitting/receiving in general, which leads to new challenges in the physical layer design of RIS wireless systems. In this paper, we provide an overview over the RIS based wireless systems, including the reflection principle, channel estimation, and system design. In particular, two types of emerging RIS systems are considered: RIS aided wireless communications (RAWC) and RIS based information transmission (RBIT), where the RIS plays the role of the reflector and the transmitter, respectively. We also envision the potential applications of RIS in 6G networks.

Keywords Reconfigurable intelligent surface, channel estimation, RIS aided wireless communications, RIS based information transmission, 6G

Citation Ying-Chang Liang, Jie Chen, Ruizhe Long, Zhen-Qing He, Xianqi Lin, Chenlu Huang, Shilin Liu, Xuemin (Sherman) Shen, and Marco Di Renzo. Reconfigurable Intelligent Surface for Smart Wireless Environment: Channel Estimation, System Design and Applications in 6G Networks. Sci China Inf Sci, for review

1 Introduction

With the wide deployment of the fifth-generation (5G) mobile communication systems, it is now a critical time to develop enabling technologies for the sixth generation (6G) communication systems. Overall, 6G systems are expected to fulfill more stringent requirements on transmission capacity, reliability, latency, coverage, energy consumption, and connection density [1–4]. The existing techniques in 5G, such as millimeter-wave (mmWave) communications, massive multi-input multi-output (MIMO), ultra-dense heterogeneous network, mainly focus on the system design at the transmitter and receiver sides, the purpose of which is to cope with the unfavorable wireless propagation environment. Recently, reconfigurable intelligent surface (RIS), also called intelligent reflecting surface, has emerged as a promising technology for its capability of configuring a wireless propagation environment [5–19]. Such technology provides designers with additional degree of freedom to fulfill the stringent requirements of 6G.

In particular, RIS is a two-dimensional array with a large number of reflective elements (REs), each of which can introduce a reflection response for the incident electromagnetic wave. Hence, by smartly adjusting the reflection coefficients of these REs with a preprogrammed controller, the reflected signals

* Corresponding author (email: liangyc@ieee.org)

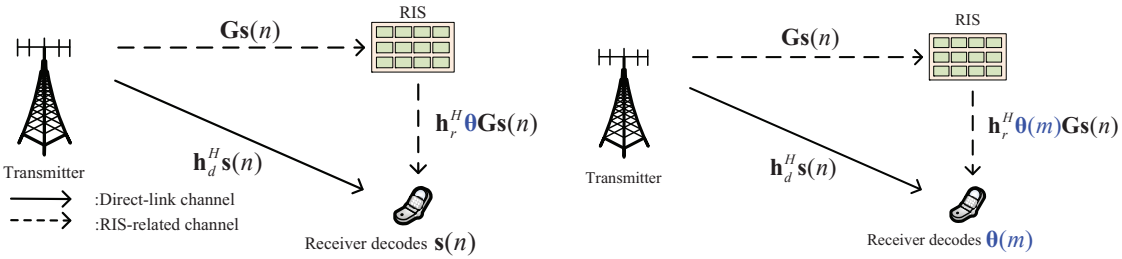

(a) RIS aided wireless communications (RAWC). (b) RIS based information transmission (RBIT).

Figure 1 Two communication paradigms of RIS. The RIS in (a) assists the transmitter to deliver $\mathbf{s}(n)$ to the receiver by adjusting its reflection coefficient matrix $\boldsymbol{\theta}$ according to the CSI, while the RIS in (b) delivers its own message to the receiver by proactively varying its reflection coefficient matrix $\boldsymbol{\theta}(m)$. The receiver in (a) aims to decode the messages embedded in $\mathbf{s}(n)$, while the receiver in (b) aims to decode the messages embedded in $\boldsymbol{\theta}(m)$ and possible $\mathbf{s}(n)$ depending on its decoding strategy. The transmitter-receiver, transmitter-RIS, and RIS-receiver channels are denoted by $\mathbf{h}_d^H$, $\mathbf{G}$, and $\mathbf{h}_r^H$, respectively.

can propagate in a desired way towards the intended receivers. As a result, the wireless environment becomes controllable and programable. Specifically, RIS can be utilized to implement two promising communication paradigms, i.e., RIS aided wireless communications (RAWC) and RIS based information transmission (RBIT).

In RAWC, RIS acts as a reflector to make the desired signal combination or interference cancellation at the intended receivers, thereby assisting the existing transmissions with higher spectrum-/energy-efficiency. Compared with existing amplify-and-forward (AF) relay aided communications [14, 20, 21], RIS is a more energy-/cost-efficient technique, because RIS reflects the incident signals passively without requiring power-consuming radio frequency (RF) components, i.e., converters and oscillators.

In RBIT, RIS acts as an information transmitter and modulates its own messages over the existing modulated or unmodulated RF radio wave generated by others [22, 23]. By proactively varying the reflection coefficients of the RIS based on specific reflection patterns, the intended receiver can detect these artificial variations and decode the embedded messages encoded by the RIS. Compared with conventional backscatter communications [24–28], the use of extremely large number of REs at the RIS helps to enhance the desired RF source, and greatly improves the performance of backscatter communications [29]. Moreover, the collaboration between the RIS information transmission and active primary transmission yields mutually beneficial spectrum and energy sharing, and such system is also termed symbiotic radio (SR) [29, 30].

RIS builds a controllable and software-defined wireless environment, and extends the frontiers of wireless communication design, offering novel solutions to 6G. For its promising capability, there are intensive research activities on RIS in the past few years, and several tutorial and survey papers have appeared in the literature. Specifically, the review paper [5] provides an overview over the reflective basics and the implementations of RIS, and it also introduces the technology evolving path of various reflective radio technologies including reflective array, backscatter communications, ambient backscatter, and RIS. The review paper [6] provides the antenna design, prototyping and experimental results of RIS, and the review papers [7–13] provide an overview of RIS technology and its applications in typical wireless communication scenarios. The survey paper [14] focus on the discussion of the differences and similarities between relays and RISs. The tutorial papers [15–17] focus on the channel modeling and theoretical performance of RIS assisted wireless communication systems. The survey papers [18, 19] focus on how to apply deep learning to achieve channel estimation, signal detection, and beamforming optimization in RAWC.

There are various challenges when deploying RIS into wireless communication systems since RIS has limited signal processing capability and cannot perform active transmitting/receiving in general. Differently from previous works [5–19] that are focused on RIS implementation, prototyping, and applications, this paper provides a different perspective. Specifically, we focus on the main state-of-the-art techniques to solve the fundamental problems in the physical layer of deploying RIS into wireless communication systems, such as channel estimation, joint active and passive beamforming optimization in the system design of RAWC, and passive information transmission optimization in the system design of RBIT. Besides, we envision related potential research directions in the deployment of RIS for 6G.

The rest of this paper is organized as follows: Section II introduces an overview of the RIS system. Then, Section III presents the channel estimation problem and shows the corresponding main solutions. Section IV discusses the joint active and passive beamforming optimization in the RAWC. In Section V,

Table 1 List of Abbreviations

5G	fifth-generation	6G	sixth-generation
ADC	analog-to-digital converters	AF	amplify-and-forward
AoA	angle of arrival	AO	alternative optimization
AoD	angle of departure	BS	base station
Big-AMP	bilinear generalized approximate message passing	CSI	channel state information
BSUM	block successive upper-bound minimization	CR	cognitive radio
CRLB	Cramér-Rao lower bound	DAC	digital-to-analog converters
DCCE	direct cascaded channel estimation	DFT	discrete Fourier transform
DnCNN	denoising convolutional neural network	DRL	deep reinforcement learning
SCCE	seperate cascaded channel estimation	ELPC	extremely low-power communication
ERLLC	extremely reliable and low-latency communications	FeMBB	further-enhanced mobile broadband
FPGA	Field-Programmable Gate Array	IoT	Internet-of-Things
KPI	key performance indicator	LS	least-square
MEC	mobile edge computing	MISO	multi-input single-output
MEMS	microelectromechanical system	MCU	micro-controller unit
MMSE	minimum mean-squared-error	MINLP	mixed-integer non-linear program
MIMO	multi-input multi-output	mmWave	millimeter-wave
NOMA	non-orthogonal multiple access	OFDM	orthogonal frequency division multiplexing
PARAFAC	parallel factor	PIN	positive-intrinsic-negative
PGM	projected gradient method	PSK	phase shift-keying
PCB	printed circuit board	QAM	quadrature amplitude modulation
RBIT	RIS based information transmission	RHCP	right-handed circularly polarized
RAWC	RIS aided wireless communications	RE	reflective element
RIS	reconfigurable intelligent surface	RCO	reflection coefficient based optimization
SINR	signal-to-interference-plus-noise ratio	SPC	short packet communication
SWIPT	simultaneous wireless information and power transfer	SDR	semidefinite relaxation
SR	symbiotic radio	SSCA	stochastic successive convex approximation
SNR	signal-to-noise ratio	THz	Terahertz
umMTC	ultra-massive machine-type communication	UC	upper computer
USRP	universal software radio peripheral	VLC	visible light communications

we present passive information transmission optimization in the RBIT. Finally, Section VI discusses the potential applications of RIS in 6G networks and Section VII concludes the paper.

2 RIS in Communication Systems

In this section, we first introduce the basic system models of two communication paradigms with RIS and then investigate the reflection principle of RIS.

2.1 System Models

RIS is generally regarded as a nearly-passive device, which has to leverage the existing active radio wave to operate its function. Specifically, the system model with RIS is shown in Fig. 1 and it is mainly composed of two channels, namely the direct-link channel and the RIS-related channel. The transmitter generates an active signal to send its messages to the receiver via the direct-link channel and the RIS-related channel, while the RIS varies its reflection coefficient matrix via the RIS-related channel according to the following two communication paradigms.

In Fig. 1(a), the RIS attempts to provide additional channel diversity via the RIS-related link, and the existing active transmission is therefore successfully performed even if the direct-link is blocked due to obstacles. Moreover, by properly designing the reflection coefficient matrix according to the instantaneous and/or statistical channel state information (CSI), the signal transmission can be enhanced thanks to the phase alignment of the reflected signal, which is referred to as RAWC.

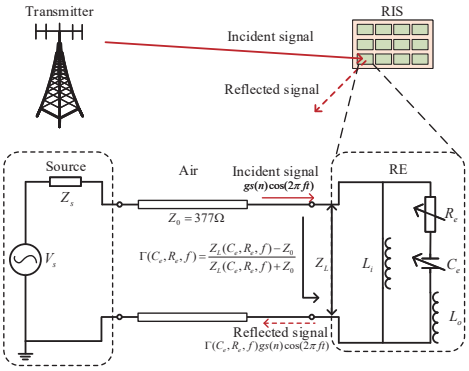

Figure 2 The equivalent circuits for the RIS reflecting element based on transmission line theory.

In Fig. 1(b), the RIS is enabled to send its own messages to the potential receiver by appropriately varying its reflection coefficients periodically, and the receiver can decode the messages from the RIS-related channel by detecting the signal variations, which is referred to as RBIT.

We evince that RIS based communications rely on the design of the reflection coefficients, it is therefore important to understand how to practically realize the tunable reflection coefficients.

2.2 Reflection Principle

In electromagnetic theory, the reflection occurs when the radio wave reaches the interface between two different media, and some part of the radio wave returns into the medium from which it is originated. For example, the reflection in RIS aided systems occurs when the incident signal from the transmitter encounters each RE at the RIS. To precisely characterize the reflected signal, it is necessary to solve Maxwell's equations by applying the boundary conditions at the interface of different media by taking into account the permittivity and permeability of the REs [31–33]. However, the calculation of Maxwell's equations is non-trivial and some simplifications are needed. In wireless engineering, when the physical size of a RE is smaller than the wavelength of the incident signal, the transmission line theory is reviewed as an adequate simplification of Maxwell's equations with the effective parameters [12]. The reflection coefficient is adopted to illustrate the ratio between the input and output electric fields with a complex number. As shown in Fig. 2, the reflection coefficient is characterized with the characteristic impedance Z_0 and the load impedance Z_L. Specifically, the characteristic impedance is a fixed value determined by the geometry and materials of the transmission line, and for the REs in the RIS, the air is regarded as the invisible transmission line with $Z_0 = 377\ \Omega$, whereas the load impedance is a reconfigurable value determined by the load circuit design. This provides a method to realize the tunable reflection coefficient by varying the load impedance.

The simplest way to change the reflection coefficients is to deploy a switch on a set of preset load impedances, which is common in the backscatter communication and low-resolution RIS. However, as the RIS has to cater to the CSI with all phase shifts as much as possible, it is highly desirable to continuously vary the phase shifts of the REs. Considering a printed circuit board (PCB)-based RIS with uniformly distributed REs on a planar surface, the RIS embeds the semiconductor, typically the positive-intrinsic-negative (PIN) diode, into the metal element in the outer layer to tune the reflection coefficients [34]. Within a given biasing voltage range, the PIN diode can be replaced with the equivalent circuit model shown in Fig. 2, where C_e and R_e are the effective capacitance and resistance, respectively. As such, the load impedance is determined by

$$Z(C_e, R_e, f) = \frac{j2\pi f L_i \left(j2\pi f L_o + \frac{1}{j2\pi C_e} + R_e\right)}{j2\pi f L_i + j2\pi f L_o + \frac{1}{j2\pi C_e} + R_e}, \tag{1}$$

where L_i, L_o, and f denote the inner layer inductance, the outer layer inductance, and the carrier frequency, respectively. Notice that the load impedance is a function with the variables C_e, R_e, and f. By varying the biasing voltage over the PIN, the load impedance is adjusted with its effective capacitance varied continuously. Consequently, the reflection coefficient can be varied continuously. However, such a design also introduces additional constraints on the reflection response. That is, the amplitude and phase cannot be independently varied [34].

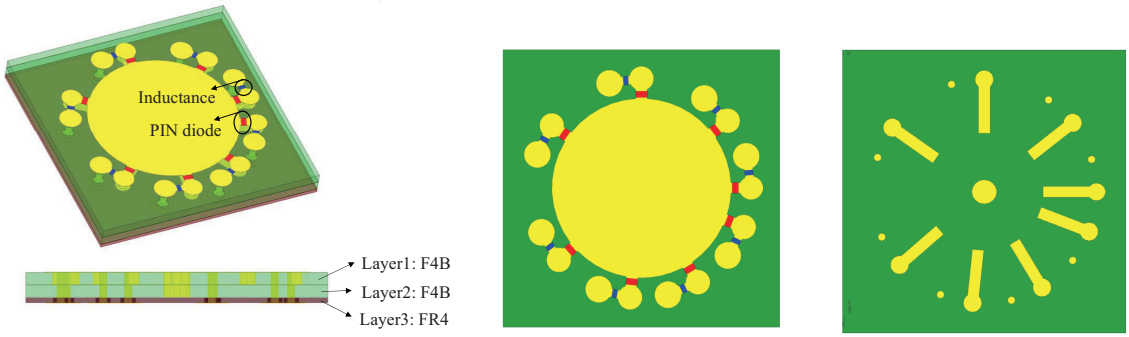

(a) Overall view of the RE. (b) Top view of Layer1. (c) Top view of Layer2.

Figure 3 Structure of the RE

2.3 The Implementation of RIS

There are also several methods proposed to reconfigure the reflection coefficients, such as loading PIN diodes [35–44], varactor diodes [45–47], and microelectromechanical system (MEMS) switches [48–50]. A PIN loaded RE was presented in [35], where the PIN can be switched at ON or OFF state to reverse the reflection phase, thus achieving 1-bit phase quantization. Then, the varactor diode was adopted in [46,47] to achieve the continuous reflection phase shift. Specifically, in [47], a RE loaded with four varactor diodes was proposed where the reflection phase can be changed continuously over 360° by controlling the biasing voltage of the varactor diode through DACs module. In addition, when the operating frequency goes to the millimeter-wave band, the MEMS switches become a promising alternative to the PIN diode, since the latter may introduce larger insertion loss. Moreover, REs loaded with liquid crystal [51, 52] and graphene [53, 54] also exhibit good performance.

To dynamically control the RIS, the system based on micro-controller unit (MCU) [41], DACs board [45–47], and Field-Programmable Gate Array (FPGA) [55–59] are usually used. In [56], the RIS is composed of 32×8 REs, each of which is loaded with two varactor diodes to achieve a reflection phase range of 45°. Then, central controller, FPGA, and DAC are utilized to generate bias voltage to tune the varactor for the desired phase distribution. The signal is then loaded on the carrier when the incident wave reflected by the RIS. Finally, a universal software radio peripheral (USRP) can be used to demodulate the received signal.

Although REs can realize the continuous reflection phase with varactors, the introduced amplitude loss is higher than that of the PIN-loaded REs. Nevertheless, the REs loaded with PIN discussed above realize at most 2-bit phase quantization. Moreover, the existing REs mainly work on linear polarization, and relatively few researches are found on the circular polarization RE with a tunable reflection phase. Then, John Huang proposed a RE composed of a rectangular patch and phase delay line [60], where the reflection phase can change with the length of the phase delay line. Based on this working principle, we propose a circularly polarized RIS with a 3-bit reconfigurable reflection phase in the range of $0° \sim 360°$. As shown in Fig. 3, PIN diodes are loaded between the circular patch and each phase delay line, where the reflection phase can be controlled by switching the on-off state of the PIN. The bias circuit of each RE is composed of eight inductors, each of which is connected to eight phase delay lines (see Fig. 3(c)), thus the quantization accuracy of the reflected phase is 45°. In addition, we model of the proposed RE in CST Studio Suite to verify its performance. By setting the right-handed circularly polarized (RHCP) plane wave incidence condition and unit cell boundary condition, the simulated reflection magnitude and phase responses of the RE are illustrated in Fig. 4. Specifically, Fig. 4(a) shows that the reflection magnitude of RE is greater than 0.75 within the range of 4.1∼4.44 GHz, and Fig. 4(b) shows that good linearity of phase response can be obtained under various working states, which is beneficial to the design of a wide-band RIS.

Then, as shown in Fig. 5(a), a RIS consisting of 8×8 the above designed REs is obtained, resulting in an aperture size of 248mm×248mm. To make the signal from the incident beam direction $(\theta_{inc}, \varphi_{inc})$ obtain a reflected radiation beam pointing to (θ_m, φ_m), the required phase compensation at the n-th RE

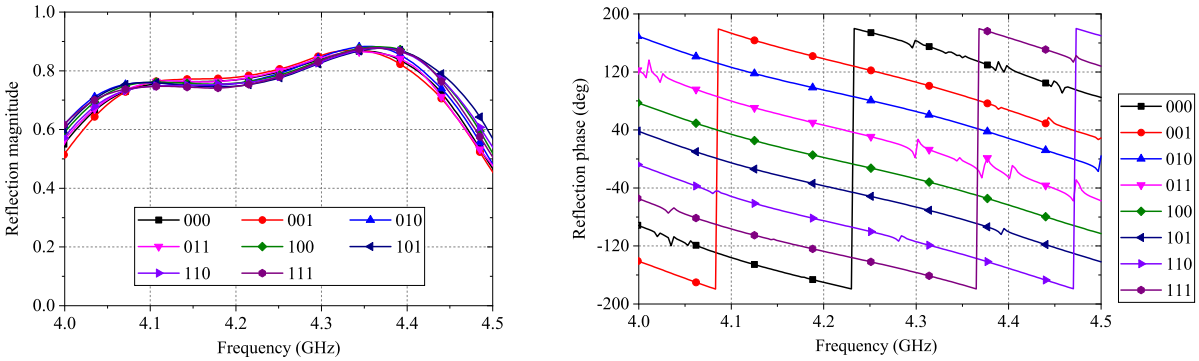

(a) Reflection magnitude response of the RE.

(b) Reflection phase response of the RE.

Figure 4 Simulated magnitude and phase response of the RE

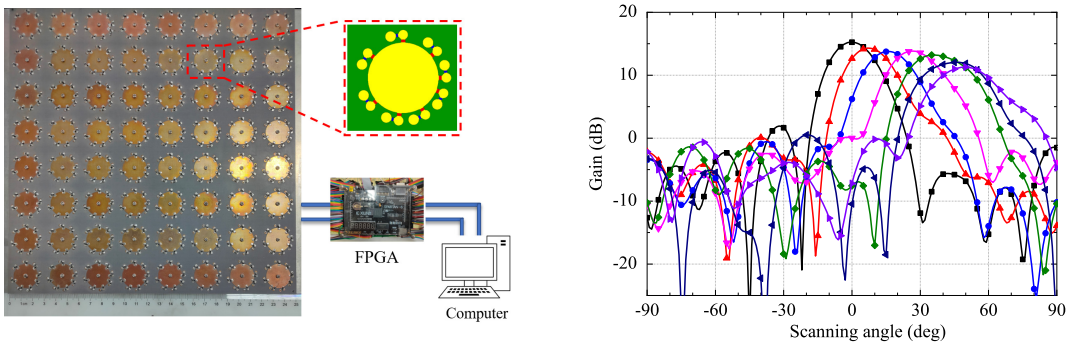

(a) Structure of the RIS.

(b) Radiation patterns of reflected beam scanning.

Figure 5 Structure of the RIS and its radiation performance.

can be calculated by [61]:

$$\phi_n = -\frac{2\pi}{\lambda}[x_n\left(\sin\theta_m\cos\varphi_m - \sin\theta_{inc}\cos\varphi_{inc}\right) + y_n\left(\sin\theta_m\sin\varphi_m - \sin\theta_{inc}\sin\varphi_{inc}\right)], \tag{2}$$

where λ is the free-space wavelength at the center frequency and (x_n, y_n) is the position of the n-th RE.

In the above RIS, the reflection phase of each RE is controlled by an upper computer (UC) through FPGA. Specifically, the UC firstly codes the designed quantized phase, and then sent it to the FPGA which connects the PIN diodes on the RIS by its output pin. Then, each PIN diode loaded on the RE is then switched to ON or OFF to get the desired phase distribution. Thus, the reflected radiation pattern can be reconfigured dynamically with different codes sent to the FPGA. Based on this control method, the simulated radiation pattern of beam scanning is shown in Fig. 5(b), from where a peak gain of 15.6dB at broadside and a beam scanning range of 50° are achieved. The simulated result verifies the excellent performance of the designed 3-bit circularly polarized RIS.

3 Channel Estimation for RIS assisted Systems

CSI acquisition is one of the main challenges for the deployment of RIS assisted systems. This is because the joint design of active beamforming at the transceiver and passive beamforming (reflection coefficient matrix) at the RIS requires the CSI of the corresponding wireless links.

In this section, we briefly introduce the fundamental channel estimation problems of RIS assisted systems. Then, we make an overview on the state-of-the-art channel estimation methods. Moreover, the advantages, disadvantages, and applicable scenarios of each method are further analyzed.

3.1 Cascaded Channel Model

Channel estimation in RIS assisted systems is more challenging than that in the traditional active device based MIMO system. This is due to the following reasons. Firstly, the CSI acquisition in the active device based system can be achieved by sending training sequences. As for RIS assisted systems, the channel estimation only can be performed at the active transceivers, since RIS is a passive device without active transmitting/receiving capabilities. Secondly, RIS is usually equipped with a large number of REs, thereby causing a high training overhead. Finally, it is quite difficult to recover the CSI of the transmitter-RIS channel and RIS-receiver channel separately, because they are coupled together with the reflection coefficient matrix.

To tackle the above challenges, researchers make efforts to find innovative methods to estimate cascaded channel, which consists of the transmitter-RIS channel and RIS-receiver channel.

Next, we investigate a typical scenario to explain the reason of estimating cascaded channels for the joint active and passive beamforming optimization in RIS assisted systems. Specifically, we consider a multi-user MISO system, where a base station (BS) equipped with multiple antennas serves multiple single-antenna users assisted by a RIS. Denote the channel responses from the BS to the RIS, from the RIS to the k-th user, and from the BS to the k-th user by $\mathbf{G}$, $\mathbf{h}_{r,k}$, and $\mathbf{h}_{d,k}$, respectively. Then, the whole channel response from BS to user k is given by $\mathbf{h}_{d,k}^H + \mathbf{h}_{r,k}^H \mathrm{diag}(\mathbf{v})\mathbf{G} = \mathbf{h}_{d,k}^H + \mathbf{v}^T \mathrm{diag}(\mathbf{h}_{r,k}^H)\mathbf{G}$ [62,63], where $\mathrm{diag}(\mathbf{v})$ is the reflection coefficient matrix. Therefore, we know the joint design of active beamforming at the BS and passive reflection coefficient matrix $\mathrm{diag}(\mathbf{v})$ at the RIS only requires the CSI of the direct-link $\mathbf{h}_{d,k}$ and the following cascaded channel, i.e.,

$$\mathbf{H}_k = \mathrm{diag}(\mathbf{h}_{r,k}^H)\mathbf{G}, \tag{3}$$

which has the bilinear structure of $\mathbf{h}_{r,k}^H$ and $\mathbf{G}$.

Note that the direct-link $\mathbf{h}_{d,k}$ can be estimated directly by setting two proper reflection coefficient matrices, i.e., arbitrary $\mathrm{diag}(\mathbf{v}_1)$ and $\mathrm{diag}(\mathbf{v}_2) = -\mathrm{diag}(\mathbf{v}_1)$ in the first and second training slots, respectively. Then, the summation of the received two training signals can cancel the reflection impacts of RIS when performing the direct-link channel estimation because of

$$\mathbf{h}_{r,k}^H \mathrm{diag}(\mathbf{v}_1)\mathbf{G} + \mathbf{h}_{r,k}^H \mathrm{diag}(-\mathbf{v}_1)\mathbf{G} = 0. \tag{4}$$

Then, the CSI of direct-link can be obtained by using the traditional estimation methods in the MIMO system.

Therefore, the main challenge of channel estimation stems from the cascaded channel estimation, which is the main objective in the recent literature. Generally, the state-of-the-art cascaded channel estimation methods can be divided into two categories based on whether or not estimating the cascaded channel directly, i.e., direct cascaded channel estimation (DCCE) and separate cascaded channel estimation (SCCE).

3.2 Separate Cascaded Channel Estimation

In this part, we introduce the SCCE method, which first separately infers the CSI of BS-RIS channel and RIS-user channel from the received training signals, and then applies them to reconstruct the cascade channels.

3.2.1 *SCCE for Semi-Passive RIS*

One straightforward method to estimate the BS-RIS channel and RIS-user channel is to insert some active channel sensors among passive REs [64] at the RIS, which is referred to as the semi-passive RIS. In [64], the typical channel sparsity is first assumed for BS-RIS channel and RIS-user channel, i.e., both of them consist of a few transmission paths, each of which depends on one path-loss scalar and the angle of arrival/departure (AoA/AoD) steering vector. Then, the BS or users can transmit pilot sequences successively to the active channel sensors at the RIS to estimate the angles and path loss of BS-RIS channel or RIS-user channels. Since the channel response of each path associated with the corresponding RE has the correlated angle and path-loss, the CSI associated with the passive REs can be recovered by applying compressive sensing and deep learning methods, thereby obtaining the full CSI of cascaded channels.

However, there are some drawbacks in the above estimator by applying the semi-passive RIS. First, the full CSI is recovered by applying the channel response correlations between REs and channel sensors, which is not applicable to uncorrelated channels, i.e., the Rayleigh fading channels. Second, the deployment of active channel sensors increases the hardware/energy cost and signal processing complexity. Furthermore, this method needs to feedback the estimated CSI to the BS or users for the joint active and passive beamforming design, which decreases the transmission efficiency.

3.2.2 *SCCE for Passive RIS*

To tackle the drawbacks of the above method, SCCE methods are further investigated in [65–67] for passive RIS without introducing any active channel sensors.

Specifically, a two-stage channel estimation method was proposed in [65, 66] for a RIS-aided single-user MIMO system, where the user transmits training sequences to the BS through RIS with different reflection coefficient matrices. Then, the received signals are rewritten in a bilinear matrix factorization form with the BS-RIS channel matrix and the composite matrix including the RIS-user channel, reflection coefficient matrix, and training sequences. In [65], an iterative algorithm was proposed to estimate the BS-RIS channel in the first stage, and the least-square (LS) estimator was applied to estimate the RIS-user channel in the second stage by applying the estimated BS-RIS channel knowledge. In [66], the channel sparsity and low-rankness of the channel matrix were further considered to reduce the training overhead. Particularly, in the first stage, the BS-RIS channel and the composite matrix were recovered from the received signals by applying the bilinear generalized approximate message passing (BiG-AMP) algorithm for sparse matrix factorization. In the second stage, the RIS-user channel was recovered from the composite matrix by applying a Riemannian manifold gradient-based algorithm for matrix completion.

Then, the channel estimation problem was extended to a RIS assisted multi-user MISO system in [67, 68]. In [67], the channel estimation problem was formulated as a matrix-calibration based matrix factorization problem. Specifically, the channels were first modeled by the Rician fading model with slow-varying and fast varying components where the slow-varying components kept quasi-static and were estimated by long-term channel averaging prior. Then, a posterior mean estimator based on Bayesian inference was derived to estimate BS-RIS channel and RIS-user channels, respectively. In [68], the anchor-assisted two-phase channel estimation scheme was proposed, where two anchor nodes were deployed near the RIS to help the channel estimation. Particularly, in the first phase, the deployed two anchor nodes transmit pilot sequences successively to estimate the element-wise channel gain square of the BS-RIS channel. Then, in the second phase, the obtained partial knowledge of BS-RIS channel is further applied to estimate RIS-user channels. Since such partial knowledge is common to all users, this estimation method is efficient for massive connection scenarios.

Moreover, the parallel factor (PARAFAC) decomposition can be also applied to perform SCCE for RIS assisted single-user [69] and multi-user systems [70]. Specifically, PARAFAC was first applied to decompose the high dimensional tensor (or matrix) into a linear combination of a number of rank-one tensors. Then, the iterative algorithms, i.e., alternating least square or vector AMP, were applied to recover the unknown channels from the decomposed forms without too much complexity.

The SCCE methods in [65–70] assume sparse, low-rank, or quasi-static channel properties when performing channel estimation for training overhead reduction. However, the matrix factorization based methods can just estimate the effective channels [66] due to the drawbacks of ambiguity when inferring the channel matrixes from a bilinear structure. Furthermore, the inaccurate BS-RIS channel and RIS-user channel estimation in the SCCE methods will produce reconstruct error when recovering the cascaded channels, thus causing higher channel estimation error and degrading the transmission efficiency.

3.3 Direct Cascaded Channel Estimation

In this part, we introduce the DCCE method, which estimates the cascaded channels directly with a properly designed channel estimation protocol.

3.3.1 *Binary Reflection based DCCE*

One straightforward method to estimate the cascaded channel directly is to turn on only one RE and keep the remaining REs off in each training slot, thus estimating the cascaded channel of each RE successively. This method is referred to as the binary reflection method, which was first proposed in [71] for a RIS

assisted single-user system. Since the RIS is usually equipped with a large number of REs, such binary reflection will cause high training overhead. In order to reduce the training overhead, this method that exploited the channel spatial correlation was further extended to a RIS assisted orthogonal frequency division multiplexing (OFDM) system with a single user [72]. Due to spatial correlation, REs can be divided into multi sub-groups, where each sub-group consisting of adjacent elements shares a common reflection coefficient. Then, the cascaded channel of each sub-group can be estimated successively by applying the binary reflection method with lower training overhead.

However, since only one RE (or one sub-group REs) works and the rest REs keep turned off, this method has the disadvantage of reducing the total power of training reflection coefficient at the RIS in each training slot, thereby decreasing estimation performance.

3.3.2 *Full Reflection based DCCE*

To tackle the drawbacks of the binary reflection method and achieve a better estimation performance, full reflection based DCCE method was further proposed in [73] based on minimizing the Cramér-Rao lower bound (CRLB), where all REs keep turned on in the whole training duration and the training reflection coefficients are designed as a discrete Fourier transform (DFT). Then, by applying the similar grouping idea in [73] to achieve overhead reduction, this method was further extended to a RIS aided OFDM single-user system with or not considering the Doppler effect in [74] and [75], respectively. However, the solutions presented in [73–75] are based on LS approach. To further improve the channel estimator based on the minimum mean-squared-error (MMSE) criterion, a deep learning based denoising convolutional neural network (DnCNN) was proposed in [76, 77] to perform DCCE, where the noisy LS channel estimation and a cleaned channel matrix are input and output.

3.3.3 *Multi-User Joint DCCE*

For a multi-user scenario, the cascaded channels of different users are correlated due to the common BS-RIS channel, which can be applied to design a multi-user joint channel estimator to achieve better performance and lower training overhead, especially for massive connection systems.

One straightforward method considering the joint channel characteristic is to apply one cascaded channel of arbitrary user with one diagonal matrix to represent the cascaded channels of all users [78–80]. For example, without loss of generality, we can use the cascaded channel of the first user, i.e., $\mathbf{H}_1$, to represent the cascaded channels of the remaining users, i.e.,

$$\mathbf{H}_k = \underbrace{\mathrm{diag}\left(\mathbf{h}_{r,k}^H\right)\mathrm{diag}\left(\mathbf{h}_{r,1}^H\right)^{-1}}_{\boldsymbol{\alpha}_k}\underbrace{\mathrm{diag}\left(\mathbf{h}_{r,1}^H\right)\mathbf{G}}_{\mathbf{H}_1} = \boldsymbol{\alpha}_k\mathbf{H}_1, \tag{5}$$

where $\boldsymbol{\alpha}_k$ is the corresponding diagonal matrix. From (5), if the common part $\mathbf{H}_1$ is already known, the rest objective only needs to estimate the diagonal matrix $\boldsymbol{\alpha}_k$. Since the number of unknown parameters in $\boldsymbol{\alpha}_k$ is much smaller than that in $\mathbf{H}_k$, the estimation of $\boldsymbol{\alpha}_k$ is much easier than that of $\mathbf{H}_k$, and the training overhead can be also reduced.

Therefore, a sequential estimation method, which first estimated the cascaded channel of one user, and then used (5) to estimate the cascaded channels of the rest users successively, was applied in [78] for a narrow-band communication system and in [79] for a wide-band communication system. Moreover, the joint channel characteristic in (5) was also investigated in [80] for a mmWave communication system. Specifically, a two-dimensional common row-column-block sparsity representation was first derived by jointly considering (5) and the channel sparsity. Then, the joint multi-user cascaded channel estimation problem was formulated as a sparse matrix recovery problem, which was further solved by a compressive sensing based two-step procedure algorithm.

4 RIS aided Wireless Communications

In RAWC, RIS acts as a reflector to induce reflection coefficients on the incident radio waves and reflect them passively. By properly designing the reflection coefficient matrix, the signals at the intended receivers can achieve signal combination or interference cancellation, thereby improving the key performance indicators (KPIs) for existing wireless communications.

In this section, we focus on the system design of the joint active beamforming at the transceiver and passive beamforming (reflection coefficient matrix) at the RIS optimization in RAWC under various practical constraints.

4.1 System Design under Ideal Case

In this part, we consider the joint active and passive beamforming under the ideal case, where the full perfect CSI can be obtained, continuous phase shifts can be achieved, phase noise can be ignored, and so on.

In fact, one of the main challenges of joint beamforming design under the ideal case is that the active and passive beamforming are coupled in the objective/constraints, which makes them non-convex. Thus, the formulated optimization problems are pretty hard to solve in general. In the following, we will illustrate the state-of-the-art solutions to tackle these challenges.

4.1.1 *Reflection Coefficient based Optimization*

This reflection coefficient based optimization (RCO) method is motivated by the fact that the optimal active beamformer at the transceiver can be directly obtained when the passive beamformer (reflection coefficient matrix) is fixed, which can be rewritten as the function of the passive beamformer. By substituting this function into the original problem, the only remaining optimization variable is the passive beamformer and the formulated problem can be solved efficiently. Specifically, the RCO method was applied to solve the transmit power minimization problem for a single-user MISO system in [63], where the semidefinite relaxation (SDR) technique was further proposed to obtain the solution of the passive beamformer. Then, the RCO method was further extended to solve a minimum signal-to-interference-plus-noise ratio (SINR) maximization problem in a multi-user MISO system [81], where the optimal passive beamformer was obtained with assuming rank one transmitter-RIS channel. However, the RCO method requires a closed-form solution of the active beamformer, which cannot be generally achieved in a complicated wireless communications system.

4.1.2 *Alternative Optimization Method*

To tackle the non-convexity challenge and the generality issue in the RCO method, most of the literature applies alternative optimization (AO) method to solve the formulated non-convex problem, where the active and passive beamformers are optimized in two independent subproblems alternatively. This method has the advantage that each subproblem can be efficiently solved with low-complexity with the remaining optimization variables being fixed. Specifically, this method was applied to solve the spectrum efficiency or energy efficiency maximization for a multi-user MISO system [82, 83], non-orthogonal multiple access (NOMA) system [84, 85], cognitive radio (CR) system [86], physical layer security [62, 87–92], active RIS aided networks [93], wireless powered communication networks [94], simultaneous wireless information and power transfer (SWIPT) systems [95], and so on.

Although the AO method is easy to implement, it updates a block of variables alternatively in each iteration, which may require many iterations to converge, especially for the scenario with a large number of REs.

4.1.3 *Projected Gradient Method*

To tackle such drawbacks of AO methods, an iterative algorithm based on the projected gradient method (PGM) was proposed in [96, 97] for a RIS aided single-user MIMO system. To solve the formulated capacity maximization problem, the optimized active and passive beamformers simultaneously move in the direction of the gradient of the objective with a determined step size iteratively. Then, the resulting solutions are projected onto the feasible region if they lie outside of the feasible set before the next iteration. This method optimizes all variables in each iteration, resulting in the faster convergence and the lower computational complexity.

4.1.4 *Deep Reinforcement Learning based Method*

Unlike the AO method which obtains the active and passive beamformers alternatively, deep reinforcement learning (DRL) based method can obtain the joint active and passive beamformer design simultaneously. In this method, by observing the predefined rewards with the continuous state and action, the joint design

is optimized through trial-and-error interactions with the environment. Specifically, DRL based methods are applied in the RIS aided multi-user systems to solve spectrum-efficiency optimization problem in [98], secure capacity optimization problem in [99], energy-efficiency optimization problem in [100], and the Terahertz communication beamforming optimization in [101].

4.2 System Design under Hardware Constraints

In this part, we introduce the system design for the RAWC under practical hardware constraints, i.e., discrete phase shifts, phase-dependent amplitude variation, and transmit/receive signal distortion.

4.2.1 *Discrete Phase Shifts*

Continuous phase shift requires infinite bits to control each RE which requires high hardware and energy cost. However, the discrete phase shifts [102] will introduce misalignment of the interest signal at the intended receivers and thus result in performance degradation. Furthermore, the formulated problem by considering the discrete phase shift in the system design is a mixed-integer non-linear program (MINLP) problem, which is NP hard in general and difficult to solve. To tackle this challenge, the joint active beamforming and passive beamforming transmission scheme was proposed in [103] to minimize the total transmit power by considering discrete phase shift, where the branch-and-bound method was proposed to obtain the optimal phase shifts for a single-user case, and then the AO method was applied to obtain the suboptimal phase shift of each RE successively for a multi-user case. Moreover, the passive beamformer jointly considering the discrete phase shifts and reflection amplitudes was studied in [104], where a new penalized Dinkelbach block successive upper-bound minimization (BSUM) method was proposed to solve the rate maximization problem for a RIS aided single-user MISO system. Specifically, numerical results in this paper show that optimizing reflection amplitude can achieve additional performance gain under the imperfect CSI scenario, which is more effective than optimizing phase shift.

4.2.2 *Phase-dependent Amplitude Variation*

The amplitude of the reflection coefficient is dependent on the phase shift of the incident wave in practical, which is minimum with zero phase shift and monotonically increases to approach unity amplitude with phase shift π or $-\pi$ [105]. This is because when the phase shift approaches zero, the image currents are in-phase with the reflecting element currents, thereby enhancing the electric field and the current flow in each RE. Then, the increased dielectric loss, metallic loss, and ohmic loss cause more energy consumption and lower reflection amplitude [106]. Specifically, the approximated partial power loss on the reflection amplitude $|\theta_n|$ can be written as the function of its phase shift $\angle\theta_n$ [107], i.e.,

$$|\theta_n| = (1 - |\theta|_{\min}) \left(\frac{\sin(\angle\theta_n - \phi) + 1}{2} \right)^{\alpha} + |\theta|_{\min}, \tag{6}$$

where $|\theta|_{\min}$, ϕ, and α are constants related to the specific circuit implementation.

From (6), we know the phase-dependent amplitude variation will cause performance degradation due to the misalignment of interest signal at the intended receivers. Furthermore, it also makes the joint active and passive beamforming design more difficult due to its complex expression of (6). Specifically, by considering the phase-dependent amplitude variation, the total transmit power was minimized in [107] subject to individual SINR constraints. Then, the RCO method and the AO method are applied to solve it for the single-user and multi-user MISO case, respectively. As for the optimization of passive beamforming in RCO/AO, a penalty-based method that penalized the constraint violation of passive beamforming was proposed to reformulate the problem, in which each reflection coefficient can be optimized by solving independent subproblems in parallel.

4.2.3 *Transmit/Receive Signal Distortion*

There exists transmit/receive signal distortion due to the inevitable hardware impairments in transceiver hardware such as amplifiers, oscillators, digital-to-analog converters (DACs), and analog-to-digital converters (ADCs), which causes misalignment of the interest signal and degrades the system performance. In particular, the joint beamforming design was studied in [108] to maximize the received signal-to-noise ratio (SNR) by considering transmit/receive signal distortion, which was further solved by the

RCO method. Then, to obtain the stationary solution of passive beamforming in the RCO method, a minorization-maximization algorithm was applied, which constructed a surrogate function, i.e., the lower bound of the original objective, and optimizes it in an iterative manner.

4.3 System Design under Statistical/Imperfect CSI

In this part, we consider the system design for the RAWC with statistical or imperfect CSI.

4.3.1 *Statistical CSI*

Frequently estimating CSI will degrade spectrum-/energy-efficiency. Hence, there is some literature investigating the joint active and passive beamforming design with statistical CSI [109–111]. Specifically, for a RIS aided single-user MISO system, the statistical Rician fading CSI was assumed to be available in [109], where the optimal joint beamforming design to maximize a tight upper bound of the ergodic capacity was obtained by applying RCO method. Then, without assuming any specific channel model, a model-free based passive beamforming design by applying stochastic successive convex approximation (SSCA) with RCO algorithm was proposed in [110] for average achievable rate maximization. Then, for a RIS aided single-user MIMO system in [111] by characterizing the spatial correlation of MIMO channel, the stationary solution of joint beamforming design to maximize the achievable ergodic capacity was obtained by applying the AO method.

4.3.2 *Imperfect CSI*

In practice, the CSI obtained with these channel estimation methods is usually imperfect, which will misguide the beamforming design for the active beamformer and especially passive beamformer, leading to additional performance degradation. Therefore, it is important to investigate the RIS assisted systems with a robust beamforming design. Without loss of generality, we investigate two classical imperfect CSI models, namely the worst-case model and the stochastic model.

Worst-Case Model: In the worst-case model, the CSI is assumed to be bounded within a fixed certain region. For this model, we usually care about the system performance with the worst-case channel conditions. For example, the robust joint active and passive beamforming design was studied in [112] for a multi-user MISO system and in [113] for a multi-user MISO CR system, where the AO method was applied to deal with the coupled active and passive beamformer and S-procedure was proposed to handle the non-convexity term of channel capacity/SNR stemming from the channel uncertainty. Besides, the tradeoff between the training overhead and energy efficiency was investigated in [114] for a singl-user MIMO system, where the joint active and passive beamforming, transmit power and bandwidth were optimized.

Stochastic Model: In the stochastic model, the CSI uncertainty is assumed as a random variable with prior knowledge on distribution. For this model, we usually care about the system performance with its outage probability. For example, the robust joint active and passive beamforming design was studied to minimize total transmission power subject to the individual outage probability constraint for a RIS aided multi-user MIMO system, where S-procedure and SSCA were applied in [115] and [116], respectively, to tackle the non-convex terms of outage probability. Besides, the statistical information such as the distribution of the locations of the users and the distribution of the multipath channels was considered in [117] for a sum-rate maximization problem, which was solved by a two-step optimization algorithm consisting of offline phase for the long term and online phase for the short term.

a two-phase optimization process is introduced, which encompasses an offline phase (long-term and sporadic) and an online (shortterm and more frequent) phase.

5 RIS based Information Transmission

In RBIT, RIS acts as an information transmitter and modulates its own messages over the existing RF radio wave by proactively varying its reflection coefficients with specific reflection patterns, thereby the targeted receiver is able to detect these artificial variations to decode the embedded messages from RIS [22, 23].

Note that RBIT is achieved via passive reflection, which is free from power-consuming active components to generate the RF carrier, including oscillators, up-converters, and power amplifiers. Besides,

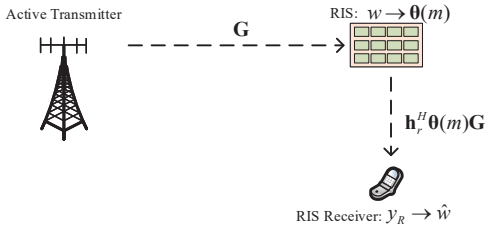

Figure 6 RBIT with unmodulated signals: The active transmitter provides the RIS with the unmodulated signals as the RF carrier.

although RIS has limited signal processing ability to achieve high order modulation and complex coding schemes, the large deployment of the REs still provides considerable spatial multiplexing or substantial diversity. Thus, the RIS-based transmitter has a great potential to achieve highly reliable communications in a spectrum-/energy-efficient manner.

In this section, motivated by the above potential advantages, we focus on the system design of RBIT under modulated and unmodulated signals in the RF radio wave.

5.1 RIS based Transmitter with Unmodulated Signals

In this part, we mainly investigate the RBIT with the unmodulated signals. As shown in Fig. 6, the RIS wants to transmit its message w to the RIS receiver by leveraging the RF carrier emitted from the active transmitter. In particular, the active transmitter equipped with a single RF chain radiates a monotone RF signal towards RIS. Then, the RIS-based transmitter directly reflects the monotone signal with the amplitude and phase variations according to its transmit symbol, thus achieving the signal modulation in the current RF frequency. During this processing, no additional RF chain but the one deployed at the active transmitter is needed, resulting in a single RF-chain transmitter. It is different from the general communication system where the number of RF chains is equal to the number of transmitter antennas. Besides, the transmission scheme is similar to backscatter communication which usually realizes the point-to-point transmission with a single RE, and however the RIS-based transmitter is able to support multi-user transmission simultaneously with the extended transmission range due to the larger number of REs. To achieve this reliable transmission, it is therefore of great significance to design the proper mapping between the message symbol and the reflecting pattern, or equivalently modulation scheme, with hardware-constrained REs.

As aforementioned, it is thought that the REs usually vary the phase of the incident signal. Elaborating its phase-shift ability, the RIS-based transmitter can easily achieve the phase shift-keying (PSK) modulation. To realize this, the RIS first optimizes its induced phases to maximize the received SNR, and then introduces additional phase variations to make the received signal aligned with the same phase shift, creating a virtual bi-dimensional M-ary signal constellation diagram at the receiver [118]. The prototype of RIS-based transmitter with 8×32 REs in [119] was proposed to achieve a high data rate transmission with 8-PSK. Furthermore, the receive antenna indices were exploited to improve the spectral efficiency with index modulation [120]. In spite of the phase modulation, the RIS-based transmitter could also achieve quadrature amplitude modulation (QAM) with a time-varying reflection coefficient [121]. Later on, the authors investigated the feasibility of using RIS for MIMO transmission with the above QAM scheme [122], which also showed the great potential to achieve high spectral efficiency with the low-cost RIS-based transmitter.

In addition to supporting a single user with high rate transmission, the RIS-based transmitter is able to serve multiple users at the same time. However, compared with the traditional MIMO transmitter design, it is more challenging to manage the user interference with the unit-modulus constraint. These powerful precoding designs, like zero forcing, maximal ratio transmission, cannot be directly adopted due to the hardware limitation of RIS. To tackle this problem, the authors in [123] considered a multi-users downlink precoding optimization problem and proposes an auto-scaled unit-modulus LS based iterative algorithm. To fully exploit the flexibility of RIS, the RIS-based transmitter adopted constructive symbol-level precoding to turn the harmful multi-user interference into a beneficial signal component [124].

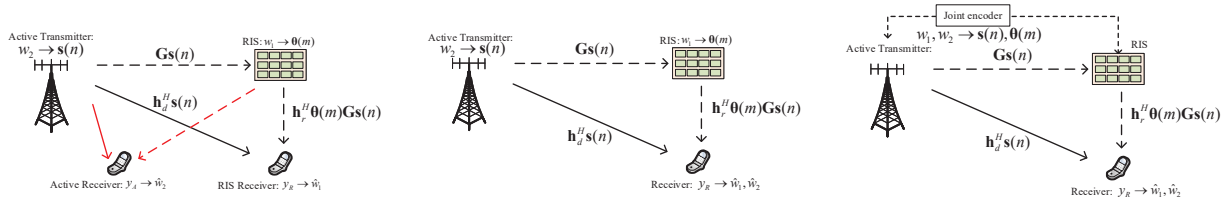

(a) **Interference**: The active transmitter and RIS based transmitter send information to their individual receivers. The active receiver and RIS receiver only decodes their own messages.

(b) **SR with joint decoding**: The active transmitter and RIS based transmitter send the separated messages to the same receiver. The receiver jointly decodes the messages.

(c) **SR with joint encoding and decoding**: The active transmitter and RIS based transmitter send the joint messages generated by the joint encoder to the receiver. The receiver jointly decodes the messages.

Figure 7 RBIT with the modulated signals.

5.2 RIS based Transmitter with Modulated Signals

In the remaining part, we further investigate the RIS-based transmitter with the modulated signal. As shown in Fig. 7, the RIS-based transmitter embeds its message w_1 into the modulated signal which is already embedded with the active transmitter message w_2 via the reflection modulation. The receiver aims to decode the message w_1 and probably message w_2 which depends on its decoding strategy. As the active transmitter provides the modulated signal rather than the unmodulated one, the reflected signal is therefore embedded with two messages w_1 and w_2. Moreover, the receiver can also receive the signal from the active transmitter if the link between them is strong enough. Thus, the RIS-based transmission has to tackle the modulated signal smartly, otherwise it will cause additional interference to the receiver, leading to a poor performance. To solve this problem, the collaboration between the RIS-based and active transmissions is needed. In the following, we will show that as the collaboration becomes closer, the relationship between the RIS-based and active transmissions will gradually become mutualistic.

5.2.1 *Interference*

As shown in Fig. 4(a), for the worst case, there is no collaboration between the RIS-based and active transmissions. The RIS-based transmitter just exploits the unmodulated signals as an imperfect carrier signal, and the RIS receiver is designed to recover the message w_1 from the RIS only. Despite the multiple REs, this system is somehow similar to the ambient backscatter communication (AmBC) [125]. Due to lack of collaboration, the two kinds of transmissions will cause interference to each other. Especially for the RIS transmission, its performance may suffer severe direct-link interference from the active transmitter. Moreover, as the receiver has no knowledge of the symbols from the active transmitter, the RIS receiver generally adopts noncoherent detection, which has lower performance compared to coherent detection.

As for the direct-link interference problem, some literature in AmBC proposed a frequency-shifting method to avoid the direct-link interference [126, 127], and others exploited the waveform feature to cancel out the interference [24, 128]. To tackle the imperfect carrier signal, the authors in [129] exploited the large degree of freedoms in RIS to let a slave antenna only receive the direct-link signal, and thus by normalizing the signals at the other antenna, the receiver can cancel the unknown source symbols. This work achieves multi-user downlink RIS-based transmission with the commodity Wi-Fi signals. Nevertheless, the modulated carrier signal is still not so ideal that the RIS-based transmission without any collaboration undergoes unsatisfactory achievement.

5.2.2 *Symbiotic Radio*

Such mutual interference in the above subsection can be avoided via forming the SR between the RIS-based transmission and the active transmission [29, 30, 130], as the SR encourages these two kinds of transmission to collaborate with each other and achieve the mutualistic benefits together. Specifically, in SR, the active transmission system shares the spectrum and energy with the RIS-based transmission and enables the RIS to perform the reflection pattern modulation via reflecting the existing active signal. In addition, the RIS receiver is designed to have the prior knowledge on the codebooks of the two transmissions and is thus able to adopt the joint decoding to decode the message w_1 and w_2 at the same time. As the receiver decodes the message w_2 from the active transmitter, the direct-link interference can be directly canceled, and also the RIS symbol detection processing is therefore coherent. In return,

the RIS also provides the multipath diversity to the active transmission via the opportunistic reflection, thereby enhancing the active transmission.

As a newly emerging communication paradigm, the SR was first introduced in [130], and the joint decoding strategy based on maximum likelihood detection was first proposed in [131] with a single RE. However, the SR with a single RE suffers from the additional path-loss introduced by the reflection and thus has poor performance. Therefore, the RIS with a large number of REs can be exploited to improve the performance of the SR. A RIS-based SR was proposed in [30], which showed that the RIS-based SR can reduce the overall power consumption with more REs deployed at the RIS. Besides, RIS-based SR can realize more sophisticated reflection modulation schemes to support more users [132]. Spatial modulation was elaborated at the RIS to improve the transmission rate of the SR system [120].

Notice that in the above design, the RIS-based transmitter and the active transmitter are designed to encode their messages w_1 and w_2 separately. If the active transmitter is also in collaboration with the RIS via a joint encoder, the joint encoding strategy can be further exploited to encode messages w_1 and w_2 together, which is shown in Fig. 4(c). The joint encoding is naturally superior to the separate encoding, since the separate encoding is actually a special case of the joint encoding.

As expected, with the collaboration between the active and RIS-based transmissions going closer, the overall system has better overall BER and rate performance than other aforementioned schemes, which were validated via the simulation results in [133] and [134], respectively. Although these collaborations usually come at the expense of additional hardware costs and computational complexity, it provides a promising way ahead to SR, which changes the interfering spectrum sharing into mutually beneficial spectrum sharing.

6 Potential Applications in 6G Networks

As aforementioned, 6G is expected to fulfill more stringent requirements on transmission capacity, reliability, latency, coverage, energy consumption, and connection density [2, 3]. Specifically, 6G should support the following typical usage scenarios and KPIs: 1) Ultra-massive machine-type communications (umMTC): the device connectivity density is larger than 10^7 devices/km^2 [2]. 2) Extremely reliable and low-latency communications (ERLLC): the reliability should be higher than 99.9999% and the latency should be smaller than 100 us [135]. 3) Further-enhanced mobile broadband (FeMBB): the peak data rate should be at least 1 Tb/s and the user-experienced data rate should be higher than 1 Gb/s [2]. 4) Extremely low-power communications (ELPC): the energy efficiency should be ten or hundred times of 5G.

To fulfill these typical stringent requirements, various promising technologies, such as Terahertz (THz) communications, short packet communications (SPC), visible light communications (VLC), mobile edge computing (MEC), and so on, have been proposed. Moreover, RIS has the capability of building a controllable and programmable wireless environment without additional energy consumption, which brings additional degree of freedom for system design. Hence, RIS can be jointly designed with these technologies to further improve the various KPIs of 6G networks. In the following, we will show some potential applications of RIS when applying it into 6G networks.

6.1 Massive Connectivity Communications

With the rise of Internet-of-Things (IoT), umMTC will be an important usage scenario of 6G networks. However, a large number of IoT devices are usually located in a dead-zone where the transmitted signals, especially for high-frequency signals, experience deep fading. One solution to this challenge is deploying RIS into umMTC systems since it can enhance the signal transmission by applying passive beamforming. Specifically, in [136], the joint active and passive beamforming design was proposed for sum mean squared error minimization in an IoT massive access system. However, the above joint beamforming design requires CSI, but channel estimation for such a system requires higher training overhead than other massive connectivity systems due to passive RIS. In [137], the sporadic traffic pattern of machine-type communications was considered for a RIS aided multi-user MISO system with massive connectivity, where a three-stage SCCE method was proposed to achieve the joint user activity and channel estimation. Moreover, to further reduce the training overhead, how to make use of channel distribution, channel sparsity, common channel knowledge, and other information to reduce the training overhead for RIS aided massive connectivity systems is an important problem in the future to be solved.

6.2 THz Communications

THz communications operating between 100 GHz and 10 THz is considered as a key enabler for FeMBB in 6G due to the extremely large bandwidth. However, high-frequency signals are much likely blocked due to the high penetration loss and reduced diffraction effects. Hence, RIS can be deployed in THz communications to alleviate the severe propagation attenuation. Specifically, the joint hybrid precoding strategy was considered in [138] to maximize the sum-rate for RIS aided Thz communication MIMO systems. In [139], the hierarchical search codebook design was proposed to achieve a low-complexity basis of beam training for channel estimation and data transmission in the above systems. Then, in [140], the RIS was mounted on a satellite to enable signal propagation in low earth orbit satellite networks with THz communications, where the theoretical error rate expressions caused by the misalignment fading were analyzed. Besides, in [141], the joint optimization of unmanned aerial vehicle trajectory, active and passive beamforming, and power and THz sub-band allocation was studied to maximize the minimum average achievable rate of all users. Inspired by these papers, how to deploy the RIS by jointly considering the location, path-loss, and active and passive beamforming, and other system characteristics for performance enhancement is an important problem to be solved.

6.3 Short Packet Communications

SPC is one of the prominent solutions to achieve ERLLC in 6G. However, the system design of SPC with RIS assisted system is quite different from that in the conventional system due to double fading cascaded channel and the hardware impairments. Specifically, the average achievable rate and error probability were investigated in [142] for a RIS aided system with finite blocklength regime, and then the impacts of phase error due to the limited quantization levels or hardware impairments on the rate and error probability were further analyzed. Moreover, it is also necessary to reconsider the joint optimization of user transmission scheduling, data packet length, and active and passive beamforming for RIS aided systems with SPC to achieve the target transmission rate, reliability, and latency requirements.

6.4 Visible Light Communications

VLC is a promising technology to meet capacity demands of 6G since it can enable the information exchange over the unlicensed visible spectrum, which relaxes the limited RF spectrum and provides a high transmission rate with green low-power healthy services. However, the full potential performance of VLC is limited by the transmission distance, which is usually between 2m-5m. Then, the reflection pattern design of RIS was investigated in [143] to steer the incident light beam, thus mitigating intensity loss and enhancing signal transmission. In addition, the RIS assisted dual-hop VLC system was studied in [144], where the optical signal was first converted into the RF signal by a relay and then transmitted to the intended receiver through RIS. Then, the outage probability and bit error rate were further derived based on the above model.

6.5 Mobile Edge Computing

MEC is a promising technology to support high-performance low-latency services because it can enable the resource-limited devices to partially offload their computations to the nearby computing nodes deployed at the network. However, the potential benefits of MEC systems are limited due to the long-distance offloading link. It is a crucial problem to jointly design the active and passive beamformers, RIS deployment, communications and computing resource allocation of RIS aided MEC systems to further enhance the uplink offloading performance and system performance. Specifically, paper [145] provides the design challenges and solutions to the typical use cases of RIS in MEC systems including shortening processing latency, improving energy efficiency, enhancing total completed task-input bit, and secure computation offloading. Then, the total completed task-input bits of all users in a RIS assisted MEC systems was considered in [146] subject to energy budgets, where a three-step BCD algorithm was proposed to obtain the solutions of the active and passive beamformer design and the users' energy partition schemes for local computing and offloading. Furthermore, since MEC can provide rich computation resources for artificial intelligence based networks, how to jointly design the RIS with various objectives in the mobile edge learning system to achieve higher system performance is also an interesting problem.

6.6 Air-Ground Communications

A large dimensional air-ground is expected in 6G due to the expanded requirements of data transmission for aerial users. However, the channels between terrestrial users and aerial users are usually strong line-of-sight links due to the open space, which introduces high inter-cell interference and degrading the transmission performance. Specifically, the RIS placement optimization by jointly considering active and passive beamforming with multiple aerial/terrestrial users in the air-ground communications was investigated in [147] to mitigate inter-cell interference and improve the network capacity. Besides, in [148], the aerial user trajectory was further considered in the above system design problem to achieve a higher spectrum and energy efficiency.

6.7 Network Security

The strict privacy and security should be supported due to the ubiquitous and unlimited wireless connectivity in the large dimensional integrated system of 6G. Specifically, in the physical layer, RIS can provide the secure communication systems with additional communication links so as to enhance the transmission to the legitimate receivers while suppressing the transmission to the eavesdroppers [88–91]. Furthermore, the artificial noise was further introduced into the above systems to improve secure communication in [92]. Moreover, it is crucial to jointly design the RIS with other secure technologies, i.e., secure channel coding, quantum communications and computing, and deep learning algorithm to predict the potential attacks and improve data privacy and communication security.

7 Conclusions

This paper has provided an overview over the fundamental physical layer issues of the RIS assisted wireless systems, including reflection principle and channel estimation, and system designs for RAWC and RBIT. Specifically, we have summarized the main state-of-the-art solutions to each issue and briefly stated the advantages/disadvantages of these solutions. Moreover, we have envisioned the related potential applications of RIS in the 6G networks. As an emerging spectrum-/energy-/cost-efficient technique, there are still many open issues and challenges when deploying RIS into reality. We hope that this paper can be a useful handbook for researchers to find benchmark schemes and effective guidance for future research in 6G networks.

References

1 X. You, C.-X. Wang, J. Huang, X. Gao, Z. Zhang, M. Wang, Y. Huang, C. Zhang, Y. Jiang, J. Wang *et al.*, "Towards 6G wireless communication networks: Vision, enabling technologies, and new paradigm shifts," *Science China Information Sciences*, vol. 64, no. 1, pp. 1–74, 2021.

2 Z. Zhang, Y. Xiao, Z. Ma, M. Xiao, Z. Ding, X. Lei, G. K. Karagiannidis, and P. Fan, "6G wireless networks: Vision, requirements, architecture, and key technologies," *IEEE Vehicular Technology Magazine*, vol. 14, no. 3, pp. 28–41, 2019.

3 L. Zhang, Y.-C. Liang, and D. Niyato, "6G visions: Mobile ultra-broadband, super internet-of-things, and artificial intelligence," *China Commun.*, vol. 16, no. 8, pp. 1–14, 2019.

4 Y.-C. Liang, *Dynamic spectrum management: from cognitive radio to blockchain and artificial intelligence*. Springer Nature, 2020.

5 Y.-C. Liang, R. Long, Q. Zhang, J. Chen, H. V. Cheng, and H. Guo, "Large intelligent surface/antennas (LISA): Making reflective radios smart," *J. Commun. Inf. Netw.*, vol. 4, no. 2, Jun. 2019, also available at arXiv preprint arXiv:1906.06578.

6 L. Dai, B. Wang, M. Wang, X. Yang, J. Tan, S. Bi, S. Xu, F. Yang, Z. Chen, M. Di Renzo *et al.*, "Reconfigurable intelligent surface-based wireless communications: Antenna design, prototyping, and experimental results," *IEEE Access*, vol. 8, pp. 45 913–45 923, 2020.

7 Q. Wu and R. Zhang, "Towards smart and reconfigurable environment: Intelligent reflecting surface aided wireless network," *IEEE Communications Magazine*, vol. 58, no. 1, pp. 106–112, 2019.

8 S. Gong, X. Lu, D. T. Hoang, D. Niyato, L. Shu, D. I. Kim, and Y.-C. Liang, "Towards smart wireless communications via intelligent reflecting surfaces: A contemporary survey," *IEEE Communications Surveys & Tutorials*, 2020.

9 Q. Wu, S. Zhang, B. Zheng, C. You, and R. Zhang, "Intelligent reflecting surface aided wireless communications: A tutorial," *IEEE Transactions on Communications*, 2021.

10 X. Yuan, Y.-J. A. Zhang, Y. Shi, W. Yan, and H. Liu, "Reconfigurable-intelligent-surface empowered wireless communications: Challenges and opportunities," *arXiv preprint arXiv:2001.00364*, 2020.

11 M. Di Renzo, M. Debbah, D.-T. Phan-Huy, A. Zappone, M.-S. Alouini, C. Yuen, V. Sciancalepore, G. C. Alexandropoulos, J. Hoydis, H. Gacanin *et al.*, "Smart radio environments empowered by reconfigurable ai meta-surfaces: An idea whose time has come," *EURASIP Journal on Wireless Communications and Networking*, vol. 2019, no. 1, pp. 1–20, 2019.

12 M. Di Renzo, A. Zappone, M. Debbah, M. S. Alouini, C. Yuen, J. de Rosny, and S. Tretyakov, "Smart radio environments empowered by reconfigurable intelligent surfaces: How it works, state of research, and the road ahead," *IEEE J. Sel. Areas Commun.*, vol. 38, no. 11, pp. 2450–2525, 2020.

13 C. Huang, S. Hu, G. C. Alexandropoulos, A. Zappone, C. Yuen, R. Zhang, M. D. Renzo, and M. Debbah, "Holographic MIMO surfaces for 6G wireless networks: Opportunities, challenges, and trends," *IEEE Wireless Commun.*, vol. 27, no. 5, pp. 118–125, 2020.

14 M. Di Renzo, K. Ntontin, J. Song, F. H. Danufane, X. Qian, F. Lazarakis, J. De Rosny, D.-T. Phan-Huy, O. Simeone, R. Zhang *et al.*, "Reconfigurable intelligent surfaces vs. relaying: Differences, similarities, and performance comparison," *IEEE Open Journal of the Communications Society*, vol. 1, pp. 798–807, 2020.

15 Y. Liu, X. Liu, X. Mu, T. Hou, J. Xu, Z. Qin, M. Di Renzo, and N. Al-Dhahir, "Reconfigurable intelligent surfaces: Principles and opportunities," *arXiv preprint arXiv:2007.03435*, 2020.

16 W. Tang, M. Z. Chen, X. Chen, J. Y. Dai, Y. Han, M. Di Renzo, Y. Zeng, S. Jin, Q. Cheng, and T. J. Cui, "Wireless communications with reconfigurable intelligent surface: Path loss modeling and experimental measurement," *IEEE Trans. Wireless Commun.*, 2020.

17 W. Tang, X. Chen, M. Z. Chen, J. Y. Dai, Y. Han, M. Di Renzo, S. Jin, Q. Cheng, and T. J. Cui, "Path loss modeling and measurements for reconfigurable intelligent surfaces in the millimeter-wave frequency band," *arXiv preprint arXiv:2101.08607*, 2021.

18 H. Gacanin and M. Di Renzo, "Wireless 2.0: Toward an intelligent radio environment empowered by reconfigurable meta-surfaces and artificial intelligence," *IEEE Vehicular Technology Magazine*, vol. 15, no. 4, pp. 74–82, 2020.

19 A. M. Elbir and K. V. Mishra, "A survey of deep learning architectures for intelligent reflecting surfaces," *arXiv preprint arXiv:2009.02540*, 2020.

20 F. Gao, T. Cui, and A. Nallanathan, "On channel estimation and optimal training design for amplify and forward relay networks," *IEEE Trans. Wireless Commun.*, vol. 7, no. 5, pp. 1907–1916, 2008.

21 S. Yang and J.-C. Belfiore, "Towards the optimal amplify-and-forward cooperative diversity scheme," *IEEE Transactions on Information Theory*, vol. 53, no. 9, pp. 3114–3126, 2007.

22 Q. Li, M. Wen, and M. Di Renzo, "Single-RF MIMO: From spatial modulation to metasurface-based modulation," *arXiv preprint arXiv:2009.00789*, 2020.

23 S. Lin, B. Zheng, G. C. Alexandropoulos, M. Wen, M. Di Renzo, and F. Chen, "Reconfigurable intelligent surfaces with reflection pattern modulation: Beamforming design and performance analysis," *IEEE Transactions on Wireless Communications*, 2020.

24 G. Yang, Y.-C. Liang, R. Zhang, and Y. Pei, "Modulation in the air: Backscatter communication over ambient OFDM carrier," *IEEE Trans. Commun.*, vol. 66, no. 3, pp. 1219–1233, 2018.

25 G. Yang, C. K. Ho, and Y. L. Guan, "Multi-antenna wireless energy transfer for backscatter communication systems," *IEEE J. Sel. Areas Commun.*, vol. 33, no. 12, pp. 2974–2987, 2015.

26 X. Kang, Y.-C. Liang, and J. Yang, "Riding on the primary: A new spectrum sharing paradigm for wireless-powered IoT devices," *IEEE Trans. Wireless Commun.*, vol. 17, no. 9, pp. 6335–6347, 2018.

27 W. Liu, Y.-C. Liang, Y. Li, and B. Vucetic, "Backscatter multiplicative multiple-access systems: Fundamental limits and practical design," *IEEE Trans. Wireless Commun.*, vol. 17, no. 9, pp. 5713–5728, 2018.

28 R. Fara, D.-T. Phan-Huy, P. Ratajczak, A. Ourir, M. Di Renzo, and J. de Rosny, "Reconfigurable intelligent surface-assisted ambient backscatter communications–experimental assessment," *arXiv preprint arXiv:2103.08427*, 2021.

29 Y. C. Liang, Q. Zhang, E. G. Larsson, and G. Y. Li, "Symbiotic radio: Cognitive backscattering communications for future wireless networks," *IEEE Trans. Cogn. Commun. Netw.*, pp. 1–1, 2020.

30 Q. Zhang, Y.-C. Liang, and H. V. Poor, "Large intelligent surface/antennas (LISA) assisted symbiotic radio for IoT communications," *arXiv preprint arXiv:2002.00340*, 2020.

31 G. Gradoni and M. Di Renzo, "End-to-end mutual coupling aware communication model for reconfigurable intelligent surfaces: An electromagnetic-compliant approach based on mutual impedances," *IEEE Wireless Communications Letters*, 2021.

32 X. Qian and M. Di Renzo, "Mutual coupling and unit cell aware optimization for reconfigurable intelligent surfaces," *IEEE Wireless Communications Letters*, 2021.

33 A. Abrardo, D. Dardari, M. Di Renzo, and X. Qian, "MIMO interference channels assisted by reconfigurable intelligent surfaces: Mutual coupling aware sum-rate optimization based on a mutual impedance channel model," *arXiv preprint arXiv:2102.07155*, 2021.

34 S. Abeywickrama, R. Zhang, Q. Wu, and C. Yuen, "Intelligent reflecting surface: Practical phase shift model and beamforming optimization," *arXiv preprint arXiv:2002.10112*, 2020.

35 D. Wang, L. Yin, T. Huang, F. Han, Z. Zhang, Y. Tan, and P. Liu, "Design of a 1 bit broadband space-time-coding digital metasurface element," *IEEE Antennas and Wireless Propagation Letters*, vol. 19, no. 4, pp. 611–615, 2020.

36 C. Huang, B. Sun, W. Pan, J. Cui, X. Wu, and X. Luo, "Dynamical beam manipulation based on 2-bit digitally-controlled coding metasurface," *Scientific Reports*, vol. 7, p. 42302, Feb. 2017.

37 H. Xu, S. Xu, F. Yang, and M. Li, "Design and experiment of a dual-band 1 bit reconfigurable reflectarray antenna with independent large-angle beam scanning capability," *IEEE Antennas and Wireless Propagation Letters*, vol. 19, no. 11, pp. 1896–1900, 2020.

38 H. Yang, F. Yang, S. Xu, M. Li, X. Cao, and J. Gao, "A 1-bit multipolarization reflectarray element for reconfigurable large-aperture antennas," *IEEE Antennas and Wireless Propagation Letters*, vol. 16, pp. 581–584, 2016.

39 Z. Wang, Y. Ge, J. Pu, X. Chen, G. Li, Y. Wang, K. Liu, H. Zhang, and Z. Chen, "1 bit electronically reconfigurable folded reflectarray antenna based on pin diodes for wide-angle beam-scanning applications," *IEEE Transactions on Antennas and Propagation*, vol. 68, no. 9, pp. 6806–6810, 2020.

40 H. Yang, F. Yang, S. Xu, Y. Mao, M. Li, X. Cao, and J. Gao, "A 1-bit 10× 10 reconfigurable reflectarray antenna: design, optimization, and experiment," *IEEE Transactions on Antennas and Propagation*, vol. 64, no. 6, pp. 2246–2254, 2016.

41 J. Han, L. Li, G. Liu, Z. Wu, and Y. Shi, "A wideband 1 bit 12× 12 reconfigurable beam-scanning reflectarray: design, fabrication, and measurement," *IEEE Antennas and Wireless Propagation Letters*, vol. 18, no. 6, pp. 1268–1272, 2019.

42 Y. Li and A. Abbosh, "Reconfigurable reflectarray antenna using single-layer radiator controlled by pin diodes," *IET Microwaves, Antennas & Propagation*, vol. 9, no. 7, pp. 664–671, 2014.

43 H. Yang, F. Yang, X. Cao, S. Xu, J. Gao, X. Chen, M. Li, and T. Li, "A 1600-element dual-frequency electronically reconfigurable reflectarray at x/ku-band," *IEEE Transactions on Antennas and Propagation*, vol. 65, no. 6, pp. 3024–3032, 2017.

44 X. Yang, S. Xu, F. Yang, and M. Li, "A novel 2-bit reconfigurable reflectarray element for both linear and circular polarizations," in *2017 IEEE International Symposium on Antennas and Propagation & USNC/URSI National Radio Science*

Meeting. IEEE, 2017, pp. 2083–2084.
45 F. Venneri, S. Costanzo, and G. Di Massa, "Design and validation of a reconfigurable single varactor-tuned reflectarray," *IEEE Transactions on Antennas and Propagation*, vol. 61, no. 2, pp. 635–645, 2012.
46 B. Ratni, A. de Lustrac, G.-P. Piau, and S. N. Burokur, "Active metasurface for reconfigurable reflectors," *Applied Physics A*, vol. 124, no. 2, pp. 1–8, 2018.
47 M. E. Trampler, R. E. Lovato, and X. Gong, "Dual-resonance continuously beam-scanning x-band reflectarray antenna," *IEEE Transactions on Antennas and Propagation*, vol. 68, no. 8, pp. 6080–6087, 2020.
48 X. Yang, S. Xu, F. Yang, and M. Li, "Design of a 2-bit reconfigurable reflectarray element using two mems switches," in *2015 IEEE International Symposium on Antennas and Propagation & USNC/URSI National Radio Science Meeting*. IEEE, 2015, pp. 2167–2168.
49 T. Debogovic and J. Perruisseau-Carrier, "Low loss mems-reconfigurable 1-bit reflectarray cell with dual-linear polarization," *IEEE Transactions on Antennas and Propagation*, vol. 62, no. 10, pp. 5055–5060, 2014.
50 O. Bayraktar, O. A. Civi, and T. Akin, "Beam switching reflectarray monolithically integrated with rf mems switches," *IEEE Transactions on Antennas and Propagation*, vol. 60, no. 2, pp. 854–862, 2011.
51 J. Yang, P. Wang, S. Sun, Y. Li, Z. Yin, and G. Deng, "A novel electronically controlled two-dimensional terahertz beam-scanning reflectarray antenna based on liquid crystals," *Front. Phys. 8: 576045. doi: 10.3389/fphy*, 2020.
52 G. Perez-Palomino, P. Baine, R. Dickie, M. Bain, J. A. Encinar, R. Cahill, M. Barba, and G. Toso, "Design and experimental validation of liquid crystal-based reconfigurable reflectarray elements with improved bandwidth in f-band," *IEEE Transactions on Antennas and Propagation*, vol. 61, no. 4, pp. 1704–1713, 2013.
53 E. Carrasco and J. Perruisseau-Carrier, "Reflectarray antenna at terahertz using graphene," *IEEE Antennas and Wireless Propagation Letters*, vol. 12, pp. 253–256, 2013.
54 Z. Hamzavi-Zarghani, A. Yahaghi, and L. Matekovits, "Reconfigurable metasurface lens based on graphene split ring resonators using pancharatnam–berry phase manipulation," *Journal of Electromagnetic Waves and Applications*, vol. 33, no. 5, pp. 572–583, 2019.
55 L. Dong and H.-M. Wang, "Enhancing secure MIMO transmission via intelligent reflecting surface," *IEEE Trans. Wireless Commun.*, 2020.
56 W. Tang, J. Y. Dai, M. Z. Chen, K. K. Wong, X. Li, X. Zhao, S. Jin, Q. Cheng, and T. J. Cui, "Mimo transmission through reconfigurable intelligent surface: System design, analysis, and implementation," *IEEE Journal on Selected Areas in Communications*, vol. 38, no. 11, pp. 2683–2699, 2020.
57 L. Zhang, Z. X. Wang, R. W. Shao, J. L. Shen, X. Q. Chen, X. Wan, Q. Cheng, and T. J. Cui, "Dynamically realizing arbitrary multi-bit programmable phases using a 2-bit time-domain coding metasurface," *IEEE Transactions on Antennas and Propagation*, vol. 68, no. 4, pp. 2984–2992, 2020.
58 L. Li, Y. Shuang, Q. Ma, H. Li, H. Zhao, M. Wei, L. Che, C. Hao, C.-W. Qiu, and T. Cui, "Intelligent metasurface imager and recognizer," *Light: Science & Applications*, vol. 8, 12 2019.
59 X. Pan, F. Yang, S. Xu, and M. Li, "A 10 240-element reconfigurable reflectarray with fast steerable monopulse patterns," *IEEE Transactions on Antennas and Propagation*, vol. 69, no. 1, pp. 173–181, 2021.
60 J. Huang, "Microstrip reflectarray," in *Antennas and Propagation Society Symposium 1991 Digest*, London, ON, Canada, 1991, pp. 612–615 vol.2.
61 D. Berry, R. Malech, and W. Kennedy, "The reflectarray antenna," *IEEE Transactions on Antennas and Propagation*, vol. 11, no. 6, pp. 645–651, 1963.
62 J. Chen, Y.-C. Liang, Y. Pei, and H. Guo, "Intelligent reflecting surface: A programmable wireless environment for physical layer security," *IEEE ACCESS*, vol. 7, pp. 82 599 – 82 612, Jun. 2019.
63 Q. Wu and R. Zhang, "Intelligent reflecting surface enhanced wireless network via joint active and passive beamforming," *IEEE Trans. Wireless Commun.*, vol. 18, no. 11, pp. 5394–5409, 2019.
64 A. Taha, M. Alrabeiah, and A. Alkhateeb, "Enabling large intelligent surfaces with compressive sensing and deep learning," *arXiv preprint arXiv:1904.10136*, 2019.
65 J. Zhang, C. Qi, P. Li, and P. Lu, "Channel estimation for reconfigurable intelligent surface aided massive MIMO system," in *Proc. IEEE SPAWC*, 2020, pp. 1–5.
66 Z.-Q. He and X. Yuan, "Cascaded channel estimation for large intelligent metasurface assisted massive MIMO," *IEEE Wireless Commun. Lett.*, vol. 9, no. 2, pp. 210–214, 2019.
67 H. Liu, X. Yuan, and Y.-J. A. Zhang, "Matrix-calibration-based cascaded channel estimation for reconfigurable intelligent surface assisted multiuser MIMO," *IEEE J. Sel. Areas Commun.*, 2020.
68 X. Guan, Q. Wu, and R. Zhang, "Anchor-assisted intelligent reflecting surface channel estimation for multiuser communications," *arXiv preprint arXiv:2008.00622*, 2020.
69 G. T. de Araújo and A. L. de Almeida, "Parafac-based channel estimation for intelligent reflective surface assisted MIMO system," in *2020 IEEE 11th Sensor Array and Multichannel Signal Processing Workshop (SAM)*. IEEE, 2020, pp. 1–5.
70 L. Wei, C. Huang, G. C. Alexandropoulos, C. Yuen, Z. Zhang, M. Debbah *et al.*, "Channel estimation for ris-empowered multi-user miso wireless communications," *arXiv preprint arXiv:2008.01459*, 2020.
71 D. Mishra and H. Johansson, "Channel estimation and low-complexity beamforming design for passive intelligent surface assisted MISO wireless energy transfer," in *Proc. IEEE ICASSP*, 2019, pp. 4659–4663.
72 Y. Yang, B. Zheng, S. Zhang, and R. Zhang, "Intelligent reflecting surface meets OFDM: Protocol design and rate maximization," *IEEE Trans. Commun.*, 2020.
73 T. L. Jensen and E. De Carvalho, "An optimal channel estimation scheme for intelligent reflecting surfaces based on a minimum variance unbiased estimator," in *Proc. IEEE ICASSP*, 2020, pp. 5000–5004.
74 S. Sun and H. Yan, "Channel estimation for reconfigurable intelligent surface-assisted wireless communications considering doppler effect," *arXiv preprint arXiv:2010.00101*, 2020.
75 B. Zheng and R. Zhang, "Intelligent reflecting surface-enhanced OFDM: Channel estimation and reflection optimization," *IEEE Wireless Commun. Lett.*, vol. 9, no. 4, pp. 518–522, 2019.
76 N. K. Kundu and M. R. McKay, "A deep learning-based channel estimation approach for miso communications with large intelligent surfaces," in *2020 IEEE 31st Annual International Symposium on Personal, Indoor and Mobile Radio Communications*. IEEE, 2020, pp. 1–6.
77 C. Liu, X. Liu, D. W. K. Ng, and J. Yuan, "Deep residual network empowered channel estimation for irs-assisted multi-user communication systems," *arXiv preprint arXiv:2012.00241*, 2020.
78 Z. Wang, L. Liu, and S. Cui, "Channel estimation for intelligent reflecting surface assisted multiuser communications:

Framework, algorithms, and analysis," *arXiv preprint arXiv:1912.11783*, 2019.
79 B. Zheng, C. You, and R. Zhang, "Intelligent reflecting surface assisted multi-user OFDMA: Channel estimation and training design," *arXiv preprint arXiv:2003.00648*, 2020.
80 J. Chen, Y.-C. Liang, H. V. Cheng, and W. Yu, "Channel estimation for reconfigurable intelligent surface aided multi-user MIMO systems," *arXiv preprint arXiv:1912.03619*, 2019.
81 A. Kammoun, A. Chaaban, M. Debbah, M.-S. Alouini *et al.*, "Asymptotic max-min sinr analysis of reconfigurable intelligent surface assisted MISO systems," *IEEE Trans. Wireless Commun.*, 2020.
82 H. Guo, Y.-C. Liang, J. Chen, and E. G. Larsson, "Weighted sum-rate maximization for reconfigurable intelligent surface aided wireless networks," *IEEE Trans. Wireless Commun.*, vol. 19, no. 5, pp. 3064–3076, 2020.
83 C. Huang, A. Zappone, G. C. Alexandropoulos, M. Debbah, and C. Yuen, "Reconfigurable intelligent surfaces for energy efficiency in wireless communication," *IEEE Trans. Wireless Commun.*, vol. 18, no. 8, pp. 4157–4170, 2019.
84 G. Yang, X. Xu, and Y.-C. Liang, "Intelligent reflecting surface assisted non-orthogonal multiple access," in *Proc. IEEE WCNC*, 2020, pp. 1–6.
85 X. Mu, Y. Liu, L. Guo, J. Lin, and N. Al-Dhahir, "Exploiting intelligent reflecting surfaces in NOMA networks: Joint beamforming optimization," *IEEE Trans. Wireless Commun.*, vol. 19, no. 10, pp. 6884–6898, 2020.
86 L. Zhang, Y. Wang, W. Tao, Z. Jia, T. Song, and C. Pan, "Intelligent reflecting surface aided MIMO cognitive radio systems," *IEEE Trans. Veh. Technol.*, vol. 69, no. 10, pp. 11 445–11 457, 2020.
87 M. Cui, G. Zhang, and R. Zhang, "Secure wireless communication via intelligent reflecting surface," *IEEE Wireless Communications Letters*, vol. 8, no. 5, pp. 1410–1414, 2019.
88 X. Yu, D. Xu, Y. Sun, D. W. K. Ng, and R. Schober, "Robust and secure wireless communications via intelligent reflecting surfaces," *IEEE Journal on Selected Areas in Communications*, vol. 38, no. 11, pp. 2637–2652, 2020.
89 H. Shen, W. Xu, S. Gong, Z. He, and C. Zhao, "Secrecy rate maximization for intelligent reflecting surface assisted multi-antenna communications," *IEEE Communications Letters*, vol. 23, no. 9, pp. 1488–1492, 2019.
90 S. Hu, Z. Wei, Y. Cai, C. Liu, D. W. K. Ng, and J. Yuan, "Robust and secure sum-rate maximization for multiuser MISO downlink systems with self-sustainable IRS," *arXiv preprint arXiv:2101.10549*, 2021.
91 Z. Chu, W. Hao, P. Xiao, and J. Shi, "Intelligent reflecting surface aided multi-antenna secure transmission," *IEEE Wireless Communications Letters*, vol. 9, no. 1, pp. 108–112, 2019.
92 S. Hong, C. Pan, H. Ren, K. Wang, and A. Nallanathan, "Artificial-noise-aided secure MIMO wireless communications via intelligent reflecting surface," *arXiv preprint arXiv:2002.07063*, 2020.
93 R. Long, Y.-C. Liang, Y. Pei, and E. G. Larsson, "Active reconfigurable intelligent surface aided wireless communications," *IEEE Trans. Wireless Commun.*, 2021, to be published. doi:10.1109/TWC.2021.3064024.
94 B. Lyu, D. T. Hoang, S. Gong, and Z. Yang, "Intelligent reflecting surface assisted wireless powered communication networks," in *Proc. IEEE WCNC Workshops*, 2020, pp. 1–6.
95 Q. Wu and R. Zhang, "Joint active and passive beamforming optimization for intelligent reflecting surface assisted swipt under qos constraints," *IEEE J. Sel. Areas Commun.*, vol. 38, no. 8, pp. 1735–1748, 2020.
96 N. S. Perović, L.-N. Tran, M. Di Renzo, and M. F. Flanagan, "Achievable rate optimization for MIMO systems with reconfigurable intelligent surfaces," *IEEE Transactions on Wireless Communications*, 2021.
97 ——, "Optimization of RIS-aided MIMO systems via the cutoff rate," *arXiv preprint arXiv:2012.05131*, 2020.
98 C. Huang, R. Mo, and C. Yuen, "Reconfigurable intelligent surface assisted multiuser miso systems exploiting deep reinforcement learning," *IEEE J. Sel. Areas Commun.*, vol. 38, no. 8, pp. 1839–1850, 2020.
99 H. Yang, Z. Xiong, J. Zhao, D. Niyato, L. Xiao, and Q. Wu, "Deep reinforcement learning based intelligent reflecting surface for secure wireless communications," *IEEE Transactions on Wireless Communications*, 2020.
100 G. Lee, M. Jung, A. T. Z. Kasgari, W. Saad, and M. Bennis, "Deep reinforcement learning for energy-efficient networking with reconfigurable intelligent surfaces," in *ICC 2020-2020 IEEE International Conference on Communications (ICC)*. IEEE, 2020, pp. 1–6.
101 C. Huang, Z. Yang, G. C. Alexandropoulos, K. Xiong, L. Wei, C. Yuen, Z. Zhang, and M. Debbah, "Multi-hop ris-empowered terahertz communications: A drl-based hybrid beamforming design," *arXiv preprint arXiv:2101.09137*, 2021.
102 D. Li, "Ergodic capacity of intelligent reflecting surface-assisted communication systems with phase errors," *IEEE Commun. Lett.*, 2020.
103 Q. Wu and R. Zhang, "Beamforming optimization for wireless network aided by intelligent reflecting surface with discrete phase shifts," *IEEE Trans. Commun.*, vol. 68, no. 3, pp. 1838–1851, 2019.
104 M.-M. Zhao, Q. Wu, M.-J. Zhao, and R. Zhang, "IRS-aided wireless communication with imperfect csi: Is amplitude control helpful or not?" in *Proc. IEEE Globecom*, 2020, pp. 1–6.
105 S. Abeywickrama, R. Zhang, Q. Wu, and C. Yuen, "Intelligent reflecting surface: Practical phase shift model and beamforming optimization," *arXiv preprint arXiv:2002.10112*, 2020.
106 H. Rajagopalan and Y. Rahmat-Samii, "Loss quantification for microstrip reflectarray: Issue of high fields and currents," in *2008 IEEE Antennas and Propagation Society International Symposium*. IEEE, 2008, pp. 1–4.
107 M. Jung, W. Saad, M. Debbah, and C. S. Hong, "On the optimality of reconfigurable intelligent surfaces (RISs): Passive beamforming, modulation, and resource allocation," *arXiv preprint arXiv:1910.00968*, 2019.
108 H. Shen, W. Xu, S. Gong, C. Zhao, and D. W. K. Ng, "Beamforming optimization for IRS-aided communications with transceiver hardware impairments," *IEEE Trans. Commun.*, 2020.
109 Y. Han, W. Tang, S. Jin, C.-K. Wen, and X. Ma, "Large intelligent surface-assisted wireless communication exploiting statistical csi," *IEEE Trans. Veh. Technol.*, vol. 68, no. 8, pp. 8238–8242, 2019.
110 H. Guo, Y.-C. Liang, and S. Xiao, "Model-free optimization for reconfigurable intelligent surface with statistical CSI," *arXiv preprint arXiv:1912.10913*, 2019.
111 J. Zhang, J. Liu, S. Ma, C.-K. Wen, and S. Jin, "Transmitter design for large intelligent surface-assisted MIMO wireless communication with statistical CSI," in *Proc. IEEE ICC Workshops*, 2020, pp. 1–5.
112 G. Zhou, C. Pan, H. Ren, K. Wang, M. Di Renzo, and A. Nallanathan, "Robust beamforming design for intelligent reflecting surface aided MISO communication systems," *IEEE Wireless Commun. Lett.*, vol. 9, no. 10, pp. 1658–1662, 2020.
113 J. Yuan, Y.-C. Liang, J. Joung, G. Feng, and E. G. Larsson, "Intelligent reflecting surface (IRS)-enhanced cognitive radio system," in *Proc. IEEE ICC*, 2020, pp. 1–6.
114 A. Zappone, M. Di Renzo, F. Shams, X. Qian, and M. Debbah, "Overhead-aware design of reconfigurable intelligent surfaces in smart radio environments," *IEEE Transactions on Wireless Communications*, 2020.
115 J. Wang, Y.-C. Liang, S. Han, and Y. Pei, "Robust beamforming and phase shift design for IRS-enhanced multi-user MISO

downlink communication," in *Proc. IEEE ICC*, 2020, pp. 1–6.
116 M.-M. Zhao, A. Liu, and R. Zhang, "Outage-constrained robust beamforming for intelligent reflecting surface aided wireless communication," *arXiv preprint arXiv:2007.10769*, 2020.
117 A. Abrardo, D. Dardari, and M. Di Renzo, "Intelligent reflecting surfaces: Sum-rate optimization based on statistical CSI," *arXiv preprint arXiv:2012.10679*, 2020.
118 E. Basar, M. Di Renzo, J. De Rosny, M. Debbah, M. Alouini, and R. Zhang, "Wireless communications through reconfigurable intelligent surfaces," *IEEE Access*, vol. 7, pp. 116 753–116 773, 2019.
119 W. Tang, J. Y. Dai, M. Chen, X. Li, Q. Cheng, S. Jin, K. Wong, and T. J. Cui, "Programmable metasurface-based RF chain-free 8PSK wireless transmitter," *Electronics Letters*, vol. 55, no. 7, pp. 417–420, 2019.
120 E. Basar, "Reconfigurable intelligent surface-based index modulation: A new beyond MIMO paradigm for 6G," *IEEE Trans. Commun.*, vol. 68, no. 5, pp. 3187–3196, 2020.
121 J. Y. Dai, W. Tang, L. X. Yang, X. Li, M. Z. Chen, J. C. Ke, Q. Cheng, S. Jin, and T. J. Cui, "Realization of multi-modulation schemes for wireless communication by time-domain digital coding metasurface," *IEEE Trans. Antennas Propag.*, vol. 68, no. 3, pp. 1618–1627, 2020.
122 W. Tang, J. Y. Dai, M. Z. Chen, K. K. Wong, X. Li, X. Zhao, S. Jin, Q. Cheng, and T. J. Cui, "MIMO transmission through reconfigurable intelligent surface: System design, analysis, and implementation," *IEEE J. Sel. Areas Commun.*, vol. 38, no. 11, pp. 2683–2699, 2020.
123 A. Bereyhi, V. Jamali, R. R. Müller, A. M. Tulino, G. Fischer, and R. Schober, "A single-RF architecture for multiuser massive MIMO via reflecting surfaces," in *Proc. IEEE ICASSP*, 2020, pp. 8688–8692.
124 R. Liu, H. Li, M. Li, and Q. Liu, "Symbol-level precoding design for intelligent reflecting surface assisted multi-user mimo systems," in *Proc. IEEE WCSP*, 2019, pp. 1–6.
125 V. Liu, A. Parks, V. Talla, S. Gollakota, D. Wetherall, and J. R. Smith, "Ambient backscatter: wireless communication out of thin air," in *Proc. ACM Sigcomm*, vol. 43, no. 4, 2013, pp. 39–50.
126 V. Iyer, V. Talla, B. Kellogg, S. Gollakota, and J. Smith, "Inter-technology backscatter: Towards internet connectivity for implanted devices," in *Proc. ACM SIGCOMM*, 2016, pp. 356–369.
127 P. Zhang, M. Rostami, P. Hu, and D. Ganesan, "Enabling practical backscatter communication for on-body sensors," in *Proc. ACM SIGCOMM*, 2016, pp. 370–383.
128 T. L. Nguyen, Y. Shin, J. Y. Kim, and D. I. Kim, "Signal detection for ambient backscatter communication with OFDM carriers," *Sensors*, vol. 19, no. 3, p. 517, 2019.
129 H. Zhao, Y. Shuang, M. Wei, T. J. Cui, P. Del Hougne, and L. Li, "Metasurface-assisted massive backscatter wireless communication with commodity wi-fi signals," *Nature communications*, vol. 11, no. 1, pp. 1–10, 2020.
130 R. Long, Y.-C. Liang, H. Guo, G. Yang, and R. Zhang, "Symbiotic radio: A new communication paradigm for passive internet of things," *IEEE Internet Things J.*, vol. 7, no. 2, pp. 1350–1363, 2020.
131 G. Yang, Q. Zhang, and Y.-C. Liang, "Cooperative ambient backscatter communications for green internet-of-things," *IEEE Internet of Things Journal*, vol. 5, no. 2, pp. 1116–1130, 2018.
132 W. Yan, X. Yuan, Z. Q. He, and X. Kuai, "Passive beamforming and information transfer design for reconfigurable intelligent surfaces aided multiuser mimo systems," *IEEE J. Sel. Areas Commun.*, vol. 38, no. 8, pp. 1793–1808, 2020.
133 S. Guo, S. Lv, H. Zhang, J. Ye, and P. Zhang, "Reflecting modulation," *IEEE J. Sel. Areas Commun.*, vol. 38, no. 11, pp. 2548–2561, 2020.
134 R. Karasik, O. Simeone, M. Di Renzo, and S. Shamai, "Single-rf multi-user communication through reconfigurable intelligent surfaces: An information-theoretic analysis," *arXiv preprint arXiv:2101.07556*, 2021.
135 S. Nayak and R. Patgiri, "6G: Envisioning the key issues and challenges," *arXiv preprint arXiv:2004.04024*, 2020.
136 P. Mursia, V. Sciancalepore, A. Garcia-Saavedra, L. Cottatellucci, X. Costa-Pérez, and D. Gesbert, "Risma: Reconfigurable intelligent surfaces enabling beamforming for iot massive access," *IEEE Journal on Selected Areas in Communications*, 2020.
137 S. Xia and Y. Shi, "Intelligent reflecting surface for massive device connectivity: Joint activity detection and channel estimation," in *Proc. 2020 ICASSP*. IEEE, 2020, pp. 5175–5179.
138 Y. Lu and L. Dai, "Reconfigurable intelligent surface based hybrid precoding for thz communications," *arXiv preprint arXiv:2012.06261*, 2020.
139 B. Ning, Z. Chen, W. Chen, and Y. Du, "Channel estimation and transmission for intelligent reflecting surface assisted thz communications," in *ICC 2020-2020 IEEE International Conference on Communications (ICC)*. IEEE, 2020, pp. 1–7.
140 K. Tekbıyık, G. K. Kurt, A. R. Ekti, A. Görçin, and H. Yanikomeroglu, "Reconfigurable intelligent surface empowered terahertz communication for leo satellite networks," *arXiv preprint arXiv:2007.04281*, 2020.
141 Y. Pan, K. Wang, C. Pan, H. Zhu, and J. Wang, "Uav-assisted and intelligent reflecting surfaces-supported terahertz communications," *arXiv preprint arXiv:2010.14223*, 2020.
142 R. Hashemi, S. Ali, N. H. Mahmood, and M. Latva-aho, "Average rate and error probability analysis in short packet communications over ris-aided urllc systems," *arXiv preprint arXiv:2102.13363*, 2021.
143 A. R. Ndjiongue, T. Ngatched, O. A. Dobre, and H. Haas, "Re-configurable intelligent surface-based VLC receivers using tunable liquid-crystals: The concept," *arXiv preprint arXiv:2101.02369*, 2021.
144 L. Yang, X. Yan, D. B. Da Costa, T. A. Tsiftsis, H.-C. Yang, and M.-S. Alouini, "Indoor mixed dual-hop vlc/rf systems through reconfigurable intelligent surfaces," *IEEE Wireless Communications Letters*, vol. 9, no. 11, pp. 1995–1999, 2020.
145 T. Bai, C. Pan, C. Han, and L. Hanzo, "Empowering mobile edge computing by exploiting reconfigurable intelligent surface," *arXiv preprint arXiv:2102.02569*, 2021.
146 X. Hu, C. Masouros, and K.-K. Wong, "Reconfigurable intelligent surface aided mobile edge computing: From optimization-based to location-only learning-based solutions," *arXiv preprint arXiv:2102.07384*, 2021.
147 H. Hashida, Y. Kawamoto, and N. Kato, "Intelligent reflecting surface placement optimization in air-ground communication networks toward 6g," *IEEE Wireless Communications*, 2020.
148 L. Ge, P. Dong, H. Zhang, J.-B. Wang, and X. You, "Joint beamforming and trajectory optimization for intelligent reflecting surfaces-assisted uav communications," *IEEE Access*, vol. 8, pp. 78 702–78 712, 2020.